Journal of Materials Chemistry A

Accepted Manuscript

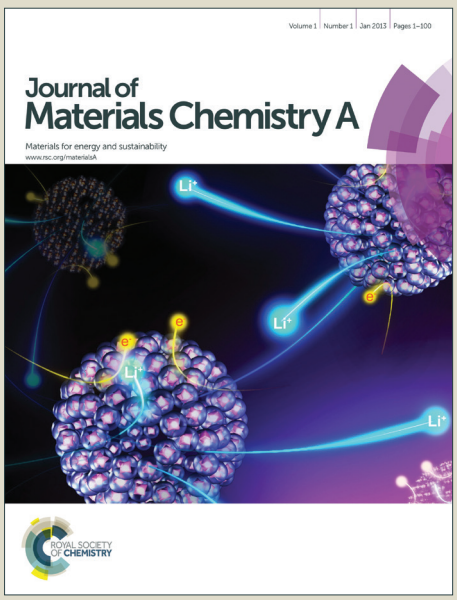

ROYAL SOCIETY OF CHEMISTRY

www.rsc.org/materialsA

J. Mater. Chem. A

RSCPublishing

ARTICLE

Templating synthesis of hollow CuO polyhedron and its application for nonenzymatic glucose detection

Cite this: DOI: 10.1039/x0xx00000x

Chuncai Kong, Linli Tang, Xiaozhe Zhang, Shaodong Sun, Shengchun Yang, Xiaoping Song and Zhimao Yang*,

Received 00th January 2012,
Accepted 00th January 2012

DOI: 10.1039/x0xx00000x

www.rsc.org/

In this report, a novel type of hollow CuO polyhedron-modified electrode for sensitive nonenzymatic glucose detection has been fabricated by a templating approach. The morphologies and structures were characterized by field-emission scanning electron microscopy (FESEM), transmission electron microscopy (TEM), X-ray diffraction (XRD), Raman spectrum and X-ray photoelectron spectroscopy (XPS). These results show that the as-prepared hollow CuO is consist of numerous CuO nanoplates. The electrochemical performance for glucose detection was investigated by cyclic voltammetry and chronoamperometry. The hollow CuO polyhedron-modified electrode exhibits a high sensitivity of 1112 μA mM^{-1} cm^{-2} with a detection limit of 0.33 μM (S/N = 3) at +0.55 V, and the linear range is up to 4 mM. Moreover, the hollow CuO polyhedron-modified electrode is also highly resistant against the interference from the interfering species such as sodium chloride (NaCl), ascorbic acid (AA) and uric acid (UA). The hollow CuO polyhedron-modified electrode exhibits high sensitivity, low detection limit, good stability and fast responce towards oxidation of glucose, thus it may be a promising nonenzymatic glucose sensor.

Introduction

In recent years, more and more attentions have been attracted on the electrochemical glucose sensor because of the significant importance for reliable and fast determination of glucose on clinical diagnostics and food industry[1-3]. In the past, glucose oxidase was usually used for the glucose detection due to its high sensitivity and selectivity[4-6]. However, the enzyme-based sensors show some disadvantages such as instability, complicated immobilization procedure and high cost[7]. Therefore, it is an important strategy to develop an excellent nonenzymatic glucose sensors. Though various metals-based nonenzymatic glucose sesors have been developed, these electrodes have such drawbacks as low selectivity, high cost and poisoning of chloride ion, which greatly limit their applications[8-13]. Hence, there is an unmet need for the development of a cheap, fast and reliable nonenzymatic glucose sensor.

Cupric oxide (CuO), as a *p*-type semiconductor with the band gap of 1.2 eV, has been widely used in catalysis[14, 15], gas sensors[16] and lithium ion batteries[17, 18]. During the past decade, many efforts have been made on nonenzymatic determination of glucose using CuO or CuO-based composite modified electrodes because of their good electrochemical activity[19-22], suggesting that CuO is a promising material as nonenzymatic glucose sensor. Various morphological CuO have been reported, such as nanoflowers[23], nanowires[14], nanorods[24], hollow nanostructures[25] and so on. Especially, hollow structures have been widely applied in sensors, catalysts and biomedicine because of their unique physical and chemical properties, including low density, interior voids, and excellent permeability[26-29]. However, there is nearly no reports about hollow CuO polyhedron. Therefore, design and synthesis of hollow CuO polyhedron is extremely demanded.

In this work, we have demonstrated the formation of hollow CuO polyhedron using Cu_2O-templated growth approach. Cu_2O is selected as templates because of its morphological multiformity, such as spherical shapes, cubes, octahedra, and other symmetric polyhedral structures[30, 31]. The electrode modified by hollow CuO polyhedron shows good electrocatalytic properties of glucose oxidation and detection. The CuO/Nafion/GCE electrode presents high sensitivity, well stability and fast amperometric response to the detection of glucose, which is promising to be an excellent nonenzymatic glucose sensor.

Experimental

Chemicals and Reagents

$Cu(CH_3COO)_2•H_2O$, sodium hydroxide (NaOH), potassium hydroxide (KOH), D-(+)-glucose, sodium chloride (NaCl), ascorbic acid (AA) and uric acid (UA) were obtained from Aladdin Reagents. Ammonium hydroxide (25%) and ethanol (99%) were obtained from Tianjin Fuyu company. All chemicals used in our experiment were of analytical grade and were used without further purification. Deionized water (18.2 MΩ·cm) was used in all preparations.

Synthesis of 26-facet Cu_2O Template

26-facet Cu_2O crystals were synthesized according to our pevious work.[31, 32] In a typical procedure, 2.9946 g of $Cu(CH_3COO)_2•H_2O$

was dissolved in 50 mL deionized water using a beaker under constant stirring at 70 ℃ for 5 min. A dark precipitate was produced when 30 mL of NaOH (3.6 g) aqueous solution was added dropwise to the above solution. After being stirred for 5 min, 0.6 g of glucose powder was added into the dark precursor with constant stirring for another 30 min at 70 ℃. Then, the obtained product were cleaned with deionized water and ethanol by repeated centrifugation, and dried at 70 ℃ for 12 h in a vacuum oven. Thus, polyhedral 26-facet Cu_2O crystals were prepared. The XRD pattern and FESEM image are shown in Fig. S1.

Synthesis of hollow CuO polyhedron

In a typical procedure, 57.6 mg of 26-facet Cu_2O powder was dispersed in a mixture solution with 10 ml of ethanol and 15 ml of deionized water, then the suspension was subjected to ultrasound for 2 min and then for another 5 min under strong stirring. Afterward, 7 ml of aqueous ammonia solution (25 wt%) was dropwise added, and the mixture was allowed to stir for 10 h at room temperature (25 ℃) 。 Lastly, the products were collected by centrifugation after different times and were dried in vacuum at 40 ℃ for further characterization.

Preparation of CuO Modified Electrode and Electrochemical Measurement

An enzyme-free amperometric electrochemical sensor was prepared by casting Nafion-impregnated CuO powders onto a glassy carbon electrode (GCE, 5 mm diameter) at room temperature. The modified electrode was prepared as follows: 1 mg of the final CuO powders were dispersed in a 1 mL of Nafion solution (0.05%, Sigma-Aldrich). After approximately 30 min of ultrasonication, 20 μL of the above suspension was dropped onto the pretreated GCE (denoted as CuO/Nafion/GCE) and dried at room temperature. Before modification, the bare GCE of 5.0 mm diameter was polished to a mirrorlike surface with 0.5 μm and 50 nm alumina slurry and then washed ultrasonically in deionized water and ethanol for a few minutes, respectively. The as-prepared CuO/Nafion/GCE was used as the working electrode with Pt foil as the counter electrode and Ag/AgCl as the reference electrode. The cyclic coltammetry (CV) measurements and chronoamperometry (CA) were performed in a 100 ml of 0.1 M KOH aqueous solution. And the CA was operated by successive injecting 100 μl of glucose into 100 ml of 0.1 M KOH aqueous solution under the potential of +0.55 V. All the measurements were carreid out at room temperature.

Instruments

The crystal phase of the as-prepared products was characterized by an X-ray diffractometer (Bruker-AXS D8 ADVANCE) using Cu-Ka radiation (λ= 1.54 Å) in the range (20–80°). The Raman spectrum was acquired using an HR 800 Raman spectrometer (HORIBA JOBIN YVON) with a CCD detector and He-Ne laser (514 nm). X-ray photoelectron spectroscopy (XPS) measurements were performed on a Kratos Axis Ultra DLD spectrometer using an Al mono Ka X-ray source.The morphology of the products was investigated by field-emission scanning electron microscopy (FESEM) using a JEOL (JSM-7000F) instrument. The transmission electron microscopy (TEM) and high resolution transmission electron microscopy (HRTEM) analysis images as well as selected-area electron diffraction (SAED) pattern analysis were performed on a JEOL JEM-2100 transmission electron microscope operating at an accelerating voltage of 200 kV. The specific surface area was determined by Brunauer-Emmett-Teller (BET) method mearsured on ASAP 2020 analyzer at 77 K. Electrochemical measurements were carried out on an Ametek VMC-4 electrochemical analyzer with a conventional three-electrode system.

Results and Discussion

Preparation of hollow CuO polyhedron

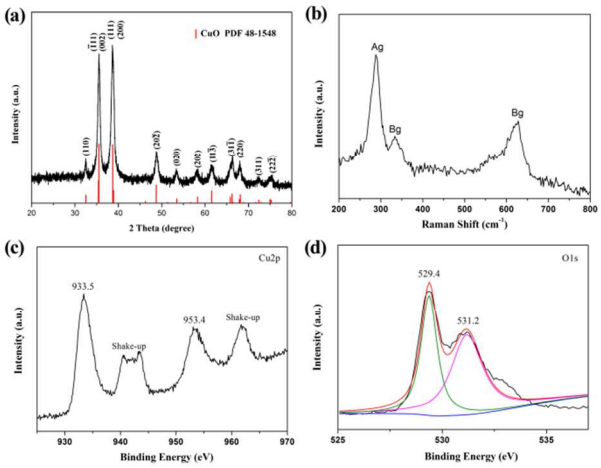

Fig. 1. (a) XRD pattern, (b) Raman spectrum, (c) Cu 2p and (d) O 1s XPS spectrum of the as-prepared products.

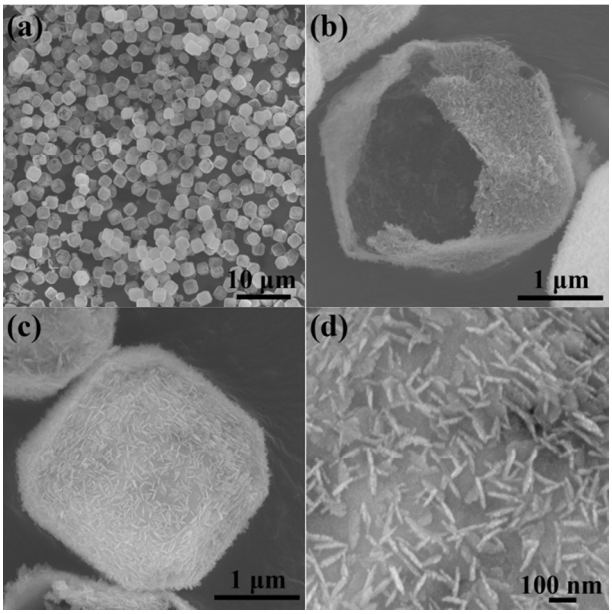

Fig.2. Typical FESEM images of the as-prepared CuO structures: (a) low-magnification; (b) and (c) individual particle; (d) high-magnification.

The crystal structure of the as-prepared hollow products was characterized by XRD, as shown in Fig. 1. All the diffraction peaks are indexed according to the standard monoclinic structure of CuO crystal (JCPDS No. 48-1548). No peaks of other inpurities are detected, suggesting the obtained products are pure CuO crystals. Fig. 1b shows the Raman spectrum of as-prepared CuO crystals. CuO belongs to the C_{2h}^6 space group with two molecules per primitive cell. Three main Raman active modes are observed at 289,

332 and 627 cm^{-1}, which is in good agreement with the previous reports[33-35]. The peak at 289 cm^{-1} can be assigned to the Ag mode, while the peaks at 332 and 627 cm^{-1} can be assigned to the Bg modes. No peaks of Cu_2O modes were found in the Raman spectrum, indicating the single phase of the CuO. The purity and the composition of the as-prepared CuO were further investigated by XPS (shown in Fig. 1c and d). As shown in Fig.1c, the peaks located at 933.5 eV and 953.4 eV are respectively assigned to core-level Cu $2p_{3/2}$ and Cu $2p_{1/2}$, corresponding to those of CuO. In addition, the strong shake-up peaks also confirm the Cu(II) oxidation state and exclude the possible existence of Cu_2O phase. As displayed in Fig.1d, the peaks observed at 529.3 eV and 531.3 eV are assigned to the lattice oxygen in CuO and the oxygen adsorbed on the surface of CuO, respectively. The Cu 2p and O 1s spectra are in good agreement with the previous reports[36, 37].

The low-magnification FESEM image (Fig. 2a) suggests that the as-prepared CuO crystals are monodisperse well and uniform in size and shape. Fig. 2b shows the image of an individual broken particle, we can see the CuO has a hollow interior. The hollow CuO crystal has a very thin shell ~120 nm. From Fig.2b and Fig.2c it can be seen that the as-prepared hollow CuO architectures consist of numerous nanoplates which makes the surface and inside rough.

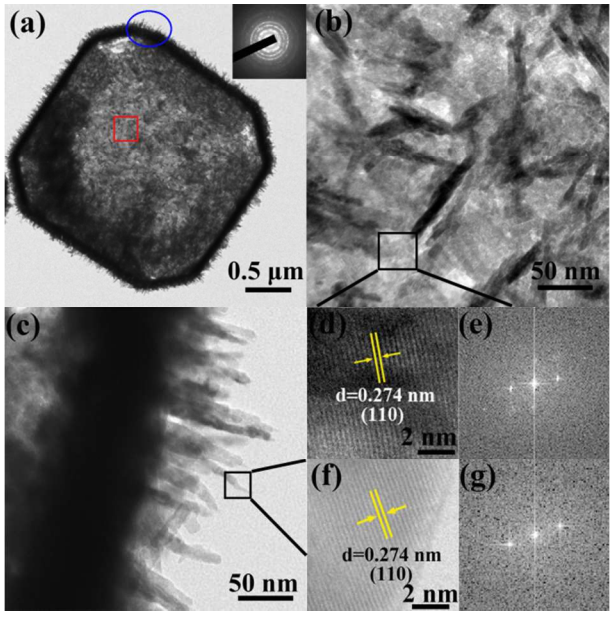

Fig.3. Typical TEM and HRTEM images of the as-prepared CuO structures: (a) individual particle, inset of (a) is the SAED pattern; (b) and (c) high-magnification; (d) and (f) HRTEM; (e) and (g) FFT images which are corresponding to (d) and (f) respectively.

The hollow interior and structure were further observed by TEM. As shown on Fig. 3a, a very obvious shell with the average thickness of 95 nm can be observed. The hollow interior and rough surface are also seen, which are corresponding to the SEM results. The inset SAED pattern of a single hollow CuO particle indicates the polycrystallinity of the product. Fig.3b shows the high-magnification image of the middle part, which is corresponding to the red box in (a). Many nanoplates can be found aggregated disorderly on the surface, and the thickness of the nanoplate is about 12 nm. The HRTEM image (Fig. 3d) and its FFT image (Fig. 3e) display that the lattice spacing is 0.274 nm, which is in good agreement with the (110) lattice spacing of CuO. Fig. 3f shows the HRTEM image of a single nanoplate, and the lattice spacing is also corresponding to the (110) of CuO.

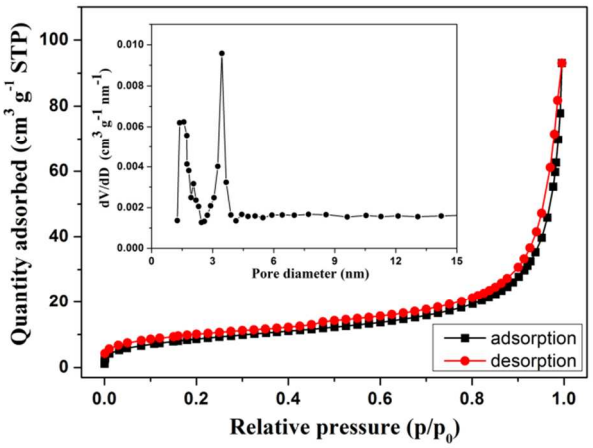

Fig. 4. Nitrogen adsorption-desorption isotherm of the hollow CuO polyhedron, the inset displays the corresponding pore size distribution obtained from the disorption curve.

The adsorption-desorption isotherm curve and the pore size distribution of as-prepared hollow CuO polyhedron are shown in Fig. 4. The Brunauer-Emmett-Teller (BET) surface area of the hollow CuO polyhedron is detected to be 31.4 m^2 g^{-1} based on the desorption curve. The pore size distribution by the Barrett-Jorner-Halenda (BJH) method displays two regions (Fig. 4 inset), 1.3 ~ 1.9 nm and 2.4 ~ 4.1 nm, which indicates the presence of micropores and mesopores with a narrow disribution. Moreover, the unique hollow structure of as-prepared products containing micropores and mesopores may make the ion diffusion to active sites more easily.[38]

The hollow CuO polyhedron was formed through the oxidative dissolution of Cu_2O in aqueous ammonia solutions and the reactions mechanism can be explained by the following four equations[25].

$$Cu_2O + 1/2\,O_2 + 2H_2O + 8NH_3 \rightarrow 2[Cu(NH_3)_4]^{2+} + 4OH^- \quad (1)$$

$$[Cu(NH_3)_4]^{2+} + 2OH^- \rightarrow Cu(OH)_2 + 4NH_3 \quad (2)$$

$$Cu(OH)_2 + 2OH^- \rightarrow Cu(OH)_4^{2-} \quad (3)$$

$$Cu(OH)_4^{2-} \rightleftharpoons CuO + 2OH^- + H_2O \quad (4)$$

When 26-facet Cu_2O crystals were added into aqueous ammonia solutions, a copper(II)-amine complex was formed from the oxidation of Cu_2O (eq.(1)). Firstly, the copper(II)-amine complex was transformed to $Cu(OH)_2$ (eq.(2)) and then a tetrahydroxo-cuprate(II) anion ($Cu(OH)_4^{2-}$) was further obtained (eq.(3)). Finally, the stable CuO was formed and precipitated (eq.(4)). The small CuO nanoparticle was firstly obtained on the surface of Cu_2O. With the increase of the reaction time, the CuO nanoparticles could further aggregate through the self-organization to form a shell. Eventually, the Cu_2O was fully consumed and the product became a CuO hollow particle. The formation of hollow CuO polyhedron can be attributed to Kirkendall effect[26, 39]. At the beginning of the reaction, a CuO shell was formed on the surface of Cu_2O. Subsequently, the O_2 and NH_3 in the solution diffused inward while the Cu^+ in Cu_2O core diffused outward. The different diffusion rates lead to the hollow structure.

Hollow CuO polyhedron modified electrode

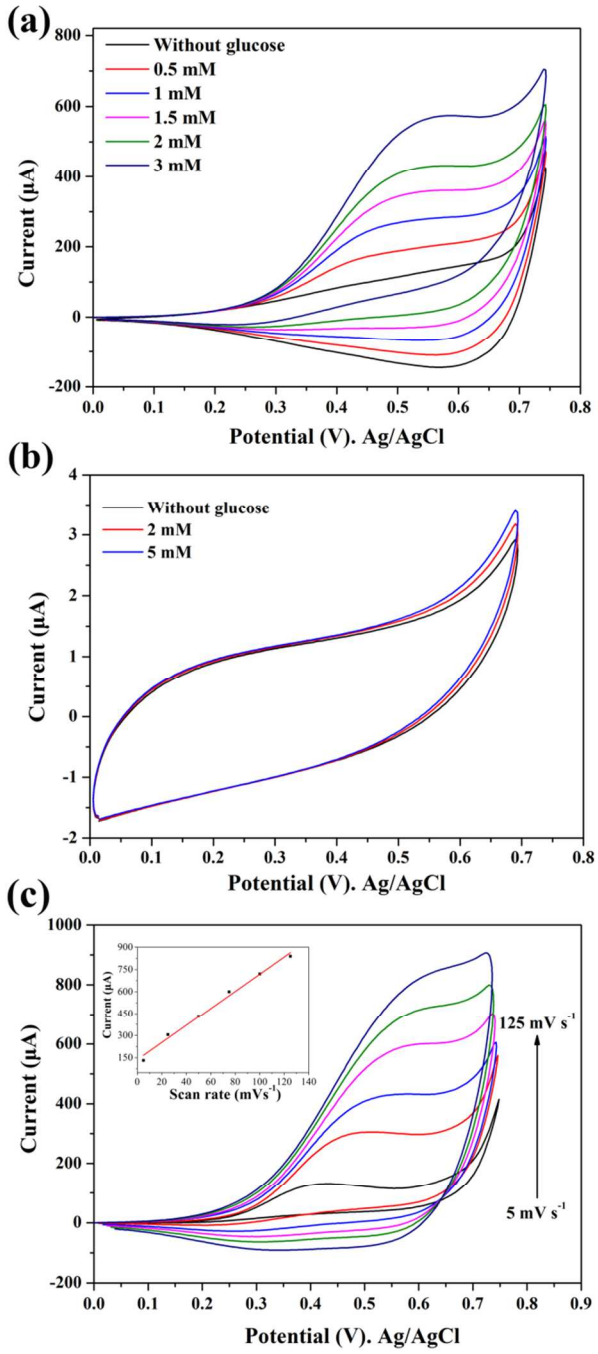

Fig. 5. (a) Cyclic voltammograms (CV) curves of hollow CuO polyhedron modified electrode (CuO/Nafion/GCE) in 0.1 M KOH solution with the concentrations of glucose from 0 to 3 mM at 50 mV s^{-1}; (b) CV curves of Nafion/GCE in 0.1 M KOH solution with the concentrations of glucose from 0 to 5 mM at 50 mV s^{-1}; (c) CV curves of CuO/Nafion/GCE at scan rates of 5 – 125 mV s^{-1} in 0.1 M KOH solution with the glucose concentration of 2 mM. Inset is the plot of oxidative peak current vs. scan rate (scanning range: 0.0 - +0.75 V).

The hollow CuO polyhedron was investigated as nonenzymatic glucose sensor and the electrocatalytic activity towards the oxidation of glucose was performed by cyclic voltammograms (CV). Figure. 5a shows the CV curves of the modified CuO/Nafion/GCE in a 0.1 M KOH solution with the concentrations of glucose from 0 to 3 mM at a scan rate of 50 mV s^{-1}. It can be seen that the current signal towards the oxidation of glucose is very weak in the absence of glucose (black curve). In contrast, theres is a very obvious peak current when glucose is added and the amperometric response increases with the enhancement of the glucose concentration. However, there are very weak current signals observed at the Nafion/GCE (see Fig.5b) either with or without glucose, proving that the activity of CuO/Nafion/GCE towards glucose is from CuO[40]. The CuO/Nafion/GCE can display a remarkable catalytic current peak at the potential of +0.55 V. So the followed chronoamperometry (CA) were performed under the potential of +0.55 V. Fig. 5c shows the effects of different scan rates on the oxidation of glucose at the CuO/Nafion/GCE electrode in 0.1M KOH solution using CV. The peaks of oxidation current increase with the increased scan rate while the peak potential shift to a more positive region. A linear relationship in the sweep range of 5 – 125 mVs^{-1} is shown , the fitting equation is I (μA) = 137.08 + 5.8051 v (mVs^{-1}) with a correlation coefficient of 0.996, which illustrates that the electrochemical kinetics are controlled by surface adsorption of glucose molecules[22].

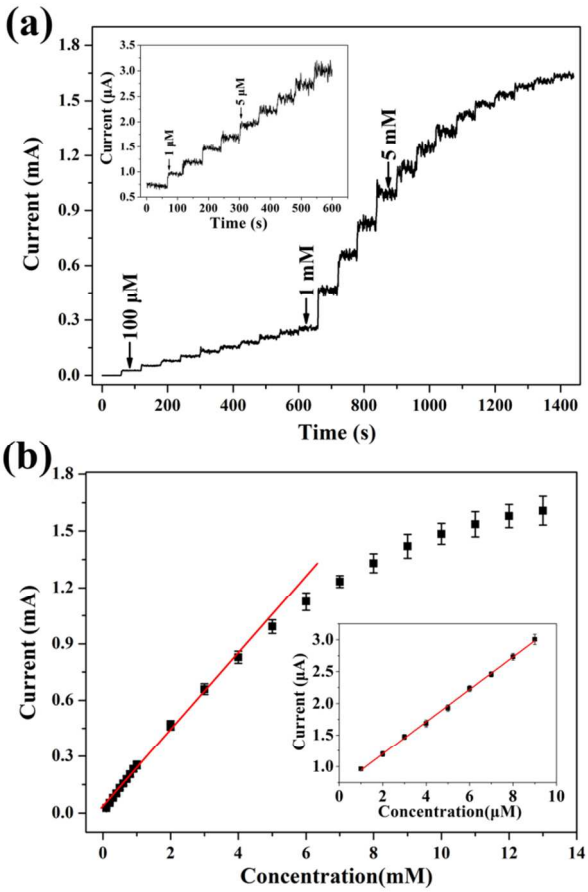

Fig. 6. (a) Amperometric response of CuO/Nafion/GCE electrode at +0.55V with a successive addition of glucose to 0.1 M KOH per 60 s. The inset shows the amperometric response at low concentrations of glucose. (b) The calibration curve of current vs. glucose concentration at the CuO/Nafion/GCE electrode. Error bars indicate standard deviations of three independent measurements by different electrodes.

Table 1. Analytical performances of the CuO/Nafion/GCE electrode with other nonenzymatic glucose sensors

Electrodes	Reference electrode	Electrolyte	Applied potential (V)	Sensitivity ($\mu A\ mM^{-1}\ cm^{-2}$)	Linear range (mM)	Detection limit (μM)	References
CuO polyhedron/Nafion/GCE	Ag/AgCl	0.1 M KOH	+ 0.55	1112	up to 4	0.33	Current work
Nafion/CuO nanospheres/GCE	Ag/AgCl	0.1 M NaOH	+ 0.6	404.5	up to 2.55	1.0	[40]
CuxO/PPy/Au	SCE	0.05 M NaOH	+ 0.6	232.22	up to 8.0	6.2	[41]
CuO/G/GCE	SCE	0.1 M NaOH	+ 0.59	1360	2 - 4	0.7	[45]
Cu-Cu_2O /Nafion/GCE	Ag/AgCl	0.1 M NaOH	+ 0.6	123.8	0.01-5.5	0.05	[42]
CuO/TiO_2	SCE	0.1 M NaOH	+ 0.5	79.79	up to 2.0	1	[43]
CuO nanoflowers/Nafion/GCE	Ag/AgCl	0.1 M KOH	+ 0.5	2657	0.01 - 5	1.71	[23]
CuxO/Cu	Ag/AgCl	0.1 M NaOH	+ 0.5	1620	up to 6.0	49	[46]
CuO nanofibers/Nafion/GCE	SCE	0.1 M NaOH	+ 0.4	431.3	0.006-2.5	0.8	[44]

GCE glassy carbon electrode; PPy polypyrrole; SCE Saturated calomel electrode; G graphene.

Amperometric repsonses of hollow CuO polyhedron towards glucose

Fig. 6a shows the amperometric response curve of the as-prepared CuO/Nafion/GCE in 0.1 M KOH solution at + 0.55 V by successive change of glucose concentrations, and the inset of Fig. 6a shows sensitive amperometric response towards lower glucose concentrations. In order to obtain an homogeneous glucose concentration the solution was vigorously stirred to guarantee good mixing of glucose with the electrolyte. There is an obvious response current signal when the glucose concentration is 100 μM. Moreover the current signal is also remarkable as the glucose concentration was diluted to 1 μM. Thus the CuO/Nafion/GCE shows a fast and sensitive response to the change of glucose concentration, and the response current increases with the enhancive glucose concentration. The signal noise increases with the enhancement of glucose concentration because of the accumulation of intermediate species on the electrode surfaces.

Fig. 6b shows the corresponding calibration curve of the CuO glucose sensor based on the amperometric results. It shows a well linear region in a range of concentrations up to 4 mM. The fitting equation is I (mA) = 0.0214 + 0.2182C (mM) with a correlation coefficient of 0.998. The non-enzymatic glucose sensor has a high sensitivity of 1112 $\mu A\ mM^{-1}\ cm^{-2}$ with a low detection limit of 0.33 μM calculated by 3σ/s, where σ and s are the standard deviation of the background current and the slope of the calibration curve, respectively. The low detection limit allows the as-prepared CuO/Nafion/GCE electrode to be suitable for the detection of blood glucose (about 4.4 ~ 6.6 mM) as well as some other biological such as urine and saliva.

For comparison, the analytical performances of the CuO/Nafion/GCE electrode with other nonenzymatic glucose sensors are listed in Table 1. It can be seen that the hollow CuO polyhedron modified electrode displays a higher sensitivity than that of CuO nanospheres (404.5 $\mu A\ mM^{-1}\ cm^{-2}$)[40], CuxO/PPy/Au (232.22 $\mu A\ mM^{-1}\ cm^{-2}$)[41], Cu-Cu_2O nanoporous (123.8 $\mu A\ mM^{-1}\ cm^{-2}$)[42], CuO/TiO_2 (79.79 $\mu A\ mM^{-1}\ cm^{-2}$)[43] and CuO nanofibers (431.3 $\mu A\ mM^{-1}\ cm^{-2}$)[44]. Though its sensitivity is lower than some nonenzymatic glucose sensors such as CuO nanocubes-graphene (1360 $\mu A\ mM^{-1}\ cm^{-2}$)[45], CuO nanoflowers (2657 $\mu A\ mM^{-1}\ cm^{-2}$)[23] and CuxO/Cu (1620 $\mu A\ mM^{-1}\ cm^{-2}$)[46], the hollow CuO polyhedron modified electrode has a lower detection limit.

Stability and anti-interference of the hollow CuO polyhedron modified electrode

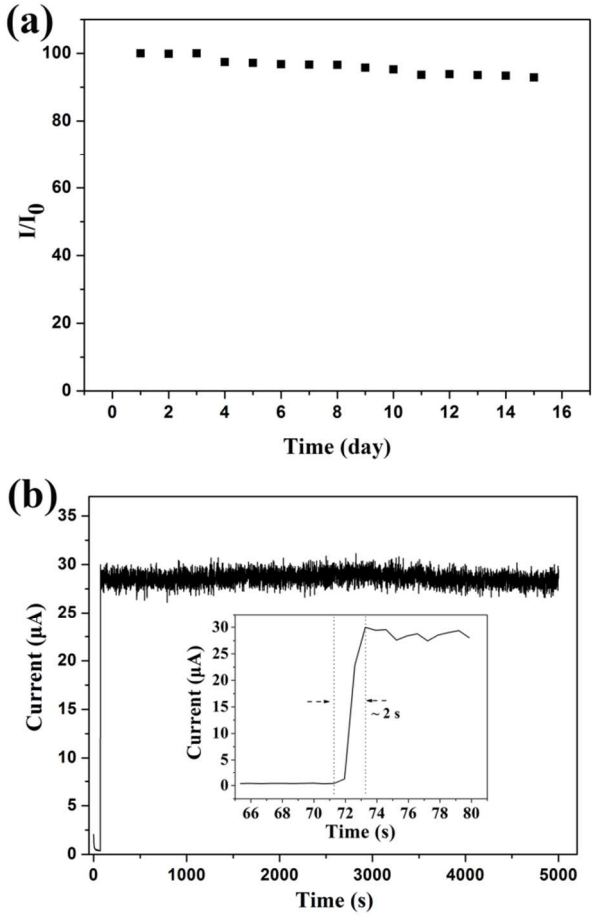

Fig. 7. (a) Long-term stability of CuO/Nafion/GCE electrode; (b) Amperometric response of CuO/Nafion/GCE electrode for 0.1 mM glucose in 0.1 mM KOH at +0.55 V over a long period of running time 4800s. Inset shows the response time of CuO/Nafion/GCE electrode to achieve a steady-state current.

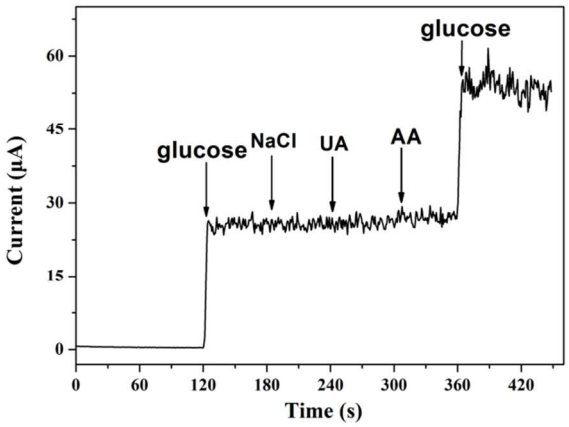

Fig. 8. Anti-Interference test of the CuO/Nafion/GCE in 0.1 M KOH solution at +0.55V with the glucose concentration of 100 μM and the interferents as indicated

The stability of the CuO/Nafion/GCE was investigated by measuring its amperometric response for a long operational period. Figure 7a displays the amperometric response to 0.1 mM glucose within a 15-day period. The CuO/Nafion/GCE electrode was exposed to air and its amperometric response was tested each day. After 15 days, the final amperometric response was approximately 93% of its original counterpart. As shown in Figure. 7b, there is nearly no loss in the current signal over a period of 80 min for 0.1 mM glucose in 0.1 M KOH at +0.55 V, suggesting the excellent stability of CuO/Nafion/GCE electrode. Moreover, the inset displays that there is no more than 2 s to achieve a steady-state current, indicating the obviously rapid response of our sensor towards glucose.

There are many easily oxidative species existed in human blood which could affect the electrochemical response, such as sodium chloride (NaCl), uric acid (UA) and ascorbic acid (AA). Herein, the anti-interference test of the above species were also studied. The normal physiological level of glucose is much higher than that of the interfering agents, so the anti-interference effect was tested by successive addition of 100 μM glucose, followed by the additions of 10 μM AA, 10 μM UA and 10 μM NaCl in a 0.1 M KOH solution, and finally another 100 μM glucose was added. As shown in Fig. 8, an obvious glucose response was observed, but there were not significant current responses for interfering species. Therefore, the hollow CuO polyhedron modified electrode shows a well selectivity selectivity for glucose detection in the presence of interfering agents.

Up to now, there is not an exact mechanism for the oxidation of glucose on the CuO modified electrode in an alkaline medium. The most accepted oxidation mechanism of glucose is that the oxidation is generated by the deprotonation of the glucose and isomerization to its enediol form [19, 23, 47, 48]. A Cu(II)/Cu(III) redox couple, which is essential factor for nonenzymatic glucose detection, is firstly formed during the reaction process (eq.(5)). After the addition of glucose, electrons are transferred from glucose to the electrode. The Cu(III) could catalyze glucose oxidation to generate gluconolactone and then gluconolactone is further oxidized to glucose acid (eq.(6)). The Cu(III) species are proposed to act as an electron-transfer medium. Thus, an enhanced catalytic current response on our CuO modified electrode in the presence of glucose solution and the response current depends on the glucose concentration. The corresponding sensing mechanism schematic is shown in Fig. 9.

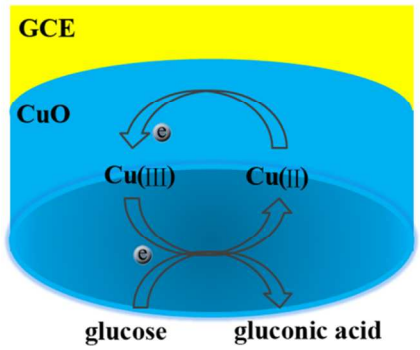

$$CuO + OH^- \longrightarrow CuOOH + e \quad (5)$$

$$CuOOH + e + glucose \longrightarrow CuO + OH^- + gluconic\ acid \quad (6)$$

Fig. 9. Schematic of the possible pathways during nonenzymatic electrooxidation of glucose on the CuO/Nafion/GCE surface in alkaline medium.

Conclutions

In summary, a Cu_2O-templated approach has been used to fabricate hollow CuO polyhedron for nonenzymatic glucose detection. The hollow CuO polyhedron modified electrode exhibites good electrocatalytic activity, high sensitivity (1112 μA mM^{-1} cm^{-2}), low detection limit (0.33 μM), wide linear range (up to 4 mM), strong stability, fast response （～ 2 s）and well selectivity toward the detection of glucose, suggensting its potential to be a candidate for the nonenzymatic detection of glucose.

Acknowledgment

This work was supported by National Science Foundation of China (NSFC No. 51272209 and 51302213), Doctoral Fund of Ministry of Education of China (No. 20120201120051), Shaanxi Province Science and Technology Innovation Team Project (No. 2013KCT-05), Youth Foundation of Shaanxi Province of China (No. 2012JQ6007), and Fundamental Research Funds for the Central Universities of China.

Notes and references

School of Science, MOE Key Laboratory for Non-Equilibrium Synthesis and Modulation of Condensed Matter, State Key Laboratory for Mechanical Behavior of Materials, Xi'an Jiaotong University, Collaborative Innovation Center of Suzhou Nano Science and Technology, Xi'an 710049, ShaanXi, People's Republic of China.. E-mail: zmyang@mail.xjtu.edu.cn

Electronic Supplementary Information (ESI) available: XRD pattern and FESEM images of the 26-facet Cu_2O. See DOI: 10.1039/b000000x/

[1] J. Wang, Chem. Rev., 2007, **108,** 814.
[2] A. Heller and B. Feldman, Chem. Rev., 2008, **108,** 2482.
[3] J. Wang, Electroanalysis, 2005, **17,** 7.
[4] H. Tang, J. H. Chen, S. Z. Yao, L. H. Nie, G. H. Deng and Y. F. Kuang, Anal. Biochem., 2004, **331,** 89.
[5] Y. H. Lin, F. Lu, Y. Tu and Z. F. Ren, Nano Lett., 2003, **4,** 191.
[6] S. Alwarappan, C. Liu, A. Kumar and C. Z. Li, J. Phys. Chem. C, 2010, **114,** 12920.

[7] J. Yang, L. C. Jiang, W. D. Zhang and S. Gunasekaran, Talanta, 2010, **82,** 25.
[8] L. Yang, Y. J. Zhang, M. Chu, W. F. Deng, Y. M. Tan, M. Ma, X. L. Su, Q. J. Xie and S. Z. Yao, Biosensors Bioelectron., 2014, **52,** 105.
[9] Y. Y. Yu, Z. G. Chen, S. J. He, B. B. Zhang, X. C. Li and M. C. Yao, Biosensors Bioelectron., 2014, **52,** 147.
[10] S. Park, T. D. Chung and H. C. Kim, Anal. Chem., 2003, **75,** 3046.
[11] X. Xiao, G. A. Montaño, T. L. Edwards, C. M. Washburn, S. M. Brozik, D. Wheeler, D. B. Burckel and R. Polsky, Biosensors Bioelectron., 2011, **26,** 3641.
[12] H. C. Gao, F. Xiao, C. B. Ching and H. W. Duan, ACS Appl. Mater. Interfaces, 2011, **3,** 3049-3057.
[13] J. P. Wang, D. F. Thomas and A.C. Chen, Anal. Chem., 2008, **80,** 997.
[14] Y. Z. Feng and X. L. Zheng, Nano Lett. 2010, **10,** 4762.
[15] Z. Y. Fei, P. Lu, X. Z. Feng, B. Sun and W. J. Ji, Catal. Sci. Technol., 2012, **2,** 1705.
[16] G. X. Zhu, H. Xu, Y. Y. Xiao, Y. J. Liu, A. H. Yuan and X. P. Shen, ACS Appl. Mater. Interfaces, 2012, **4,** 744.
[17] Y. Z Fan, R. M. Liu, W. Du, Q. Y. Lu, H. Pang and F. Gao, J. Mater. Chem., 2012, **22,** 12609.
[18] O. Waser, M. Hess, A. Güntner, P. Novák, S. E. Pratsinis, J. Power Sources, 2013, **241,** 415.
[19] S. D. Sun, X. Z. Zhang, Y. X. Sun, S. C. Yang, X. P. Song and Z. Yang, ACS Appl. Mater. Interfaces, 2013, 5, 4429.
[20] X. Wang, C. G. Hu, H. Liu, G. J. Du, X. S. He and Y. Xi, Sensor. Actuators B: Chem., 2010, **144,** 220.
[21] X. J. Zhang, G. F. Wang, X. W. Liu, J. J. Wu, M. Li, J. Gu, H. Liu and B. Fang, J. Phys. Chem. C, 2008, **112,** 16845.
[22] L. C. Jiang, W. D. Zhang, Biosensors Bioelectron., 2010, **25,** 1402.
[23] S. D. Sun, X. Z. Zhang, Y. X. Sun, S. C. Yang, X. P. Song and Z. M. Yang, Phys. Chem. Chem. Phys. 2013, **15,** 10904.
[24] L. L. Wang, H. X. Gong, C. H. Wang, D. K. Wang, K. B Tang and Y. T. Qian, Nanoscale, 2012, **4,** 6850.
[25] J. C. Park, J. Kim, H. Kwon and H. Song, Adv. Mater., 2009, **21,** 803.
[26] X.W. Lou, L.A. Archer and Z. Yang, Adv. Mater., 2008, **203,** 987.
[27] K. An, T. Hyeon, Nano Today, 2009, **4,** 359.
[28] H. W. Huang, L. Q. Zhang, K. W. Wu, Q. Yu, R. Chen, H. S.Yang, X. S. Peng and Z. Ye, Nanoscale, 2012 **4,**7832.
[29] Z. C. Wu, K. Yu, S. D. Zhang and Y. Xie, J. Phys. Chem. C, 2008, **112,** 11307.
[30] S. D. Sun, C. C. Kong, S. C. Yang, L. Q. Wang, X. P. Song, B. J. Ding and Z. M. Yang, CrystEngComm, 2011, **13,** 2217.
[31] S. D. Sun, F. Y. Zhou, L. Q. Wang, X. P. Song, B. J. Ding and Z. M. Yang, Cryst. Growth Des., 2009, **10,** 541.
[32] S. D. Sun, X. P. Song, C. C. Kong, S. H. Liang, B. J. Ding and Z. M. Yang, CrystEngComm, 2011, **13,** 6200-6205.
[33] W. Z. Wang, Q. Zhou, X. M. Fei, Y. B. He, P. C. Zhang, G. L. Zhang, L. Peng and W. J. Xie, CrystEngComm, 2010, **12,** 2232.
[34] J. F. Xu, W. Ji, Z. X. Shen, W. S. Li, S. H. Tang, X. R. Ye, D. Z. Jia and X. Q. Xin, J. Raman. Spectrosc., 1999, **30,** 413.
[35] N. Mukherjee, B. Show, S. K. Maji, U. Madhu, S. K. Bhar, B. C. Mitra, G. G. Khan and A. Mondal, Mater. Lett., 2011, **65,** 3248.
[36] H. Y. Chen, G. Z. Zhao and Y. Q. Liu, Mater. Lett., 2013, **93**, 60.
[37] J. Wang, Y. C. Liu, S. Y. Wang, X. T. Guo and Y. P. Liu, J. Mater. Chem. A, 2014, **2**, 1224.
[38] Y. C. Zhao, X. Y. Song, Q. S. Song and Z. L. Yin, CrystEngComm, 2012, **14,** 6710.
[39]M. Kong, W. Zhang, Z. Yang, S. Weng and Z. Chen, Appl. Surf. Sci., 2011, **258**, 1317.
[40] E. Reitz, W. Z. Jia, M. Gentile, Y. Wang and Y. Lei, Electroanalysis, 2008, **20,** 2482.
[41] F. H. Meng, W. Shi, Y. N. Sun, X. Zhu, G. S. Wu, C. Q. Ruan, X. Liu and D. T. Ge, Biosensors Bioelectron., 2013, **42,** 141.
[42] Y. X. Zhao, Y. P. Li, Z. Y. He and Z. F. Yan, RSC Adv. 2013, **3,** 2178.
[43] S. L. Luo, F. Su, C. B. Liu, J. X. Li, R.. H. Liu, Y. Xiao, Y. Li, X. N. Liu and Q.Y Cai, Talanta, 2011, **86,** 157.
[44] W. Wang, L. Zhang, S. Tong, X. Li, W. Song, Biosensors Bioelectron., 2009, **25,**708.
[45] L. Q. Luo, L. M. Zhu and Z. X. Wang, Bioelectrochem., 2012, **88,** 156.
[40] C. L. Li, Y. Su, S. W. Zhang, X. Y. Lv, H. L. Xia and Y. J. Wang, Biosensors Bioelectron., 2010, 26, 903.
[47] J. M. Marioli and T. Kuwana, Electrochimica Acta, 1992, **37**, 1187.
[48] J. Song, L. Xu, C. Y. Zhou, R. Q. Xing, Q. L. Dai, D. L. Liu and H. W. Song, ACS App. Mater. Interfaces, 2013, **5,** 12928.

Templating synthesis of hollow CuO polyhedron and its application for nonenzymatic glucose detection

Chuncai Kong, Lili Tang, Xiaozhe Zhang, Shaodong Sun, Shengchun Yang, Xiaoping Song and Zhimao Yang*

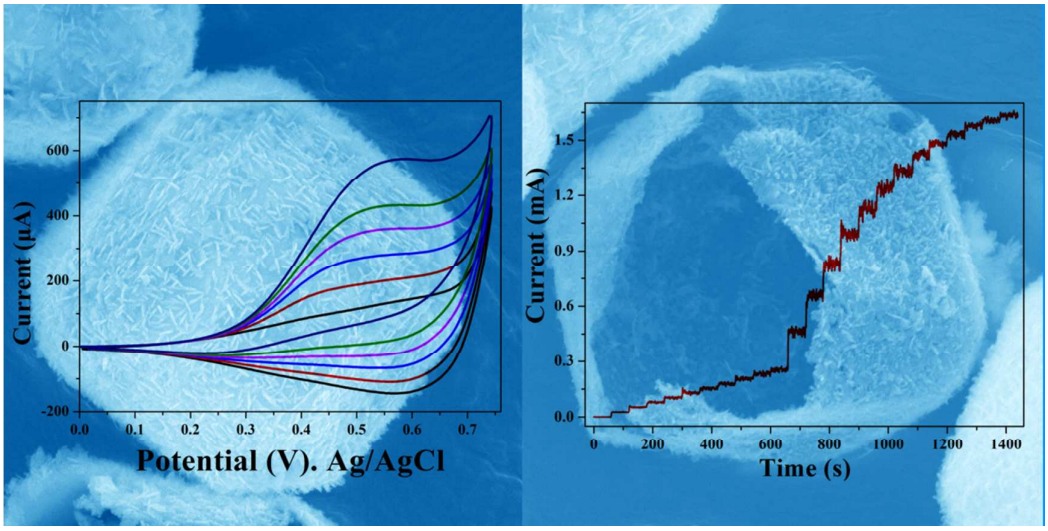

In this paper, we succesfully fabricated a novel type of hollow CuO polyhedron consist of numerous nanoplates useing Cu_2O as the templates. The hollow CuO polyhedron-modified electrode exhibits high sensitivity, low detection limit, good stability and fast responce towards the oxidation of glucose, suggesting it to be a promising nonenzymatic glucose sensor.